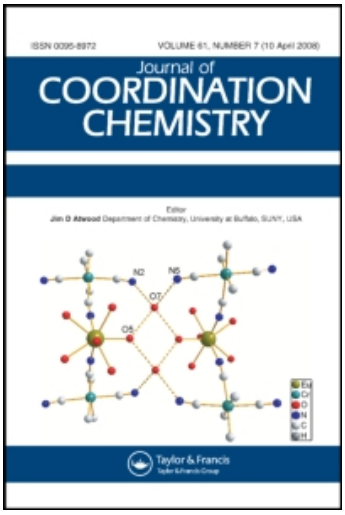

Journal of Coordination Chemistry
Publication details, including instructions for authors and subscription information:
http://www.informaworld.com/smpp/title~content=t713455674

Silver(I) 3-D-supramolecular coordination frameworks constructed by the combination of coordination bonds and supramolecular interactions

Safaa El-Din H. Etaiw[a]; Mohamed M. El-Bendary[a]
[a] Faculty of Science, Chemistry Department, Tanta University, Tanta, Egypt

Online publication date: 07 April 2010

To cite this Article Etaiw, Safaa El-Din H. and El-Bendary, Mohamed M.(2010) 'Silver(I) 3-D-supramolecular coordination frameworks constructed by the combination of coordination bonds and supramolecular interactions', Journal of Coordination Chemistry, 63: 6, 1038 — 1051
To link to this Article: DOI: 10.1080/00958971003695529
URL: http://dx.doi.org/10.1080/00958971003695529

Journal of Coordination Chemistry
Vol. 63, No. 6, 20 March 2010, 1038–1051

Taylor & Francis
Taylor & Francis Group

Silver(I) 3-D-supramolecular coordination frameworks constructed by the combination of coordination bonds and supramolecular interactions

SAFAA EL-DIN H. ETAIW* and MOHAMED M. EL-BENDARY

Faculty of Science, Chemistry Department, Tanta University, Tanta, Egypt

(*Received 27 August 2009; in final form 9 November 2009*)

Room temperature reactions of the ternary adducts of $AgNO_3$, bipodal ligand [4,4′-bipyridine (4,4′-bpy) or trans-1,2-bis(4-pyridyl)ethylene (tbpe) or 1,2-bis(4-pyridyl)ethane (bpe)] and organic ligand [4-aminobenzoic acid (4-aba) or 4-hydroxybenzoic acid (4-hba) or terephthalate ion (tph)] afford new 3-D supramolecular coordination polymers (SCPs), namely, $\{[Ag(4,4'\text{-bpy})\cdot H_2O](4\text{-ab})\cdot 2H_2O\}$ (**1**), $\{[Ag(tbpe)]0.5(4\text{-hb})\cdot 3H_2O\}$ (**2**), $[Ag_2(L)_2\cdot(tph)]$ (L = 4,4′-bpy, tbpe) (**3**,**4**) and $\{[Ag_2(bpe)_2\cdot(tph)]\cdot 2H_2O\}$ (**5**). The bipodal ligand coordinates to silver forming a 1-D cationic chain (A), while the organic ligand and solvent form a 1-D anionic chain (B) *via* hydrogen bonds. The chains construct layers which are connected *via* hydrogen bonds and π–π stacking forming a 3-D network structure. The presence of the carboxylate, amino and hydroxyl groups in the organic ligands significantly extend the dimensionality *via* hydrogen bonds. All the SCPs **1–5** exhibit strong luminescence.

Keywords: Silver supramolecular coordination polymer; Bipodal and organic ligands; π–π stacking; Hydrogen bonding

1. Introduction

Supramolecular assemblies have been achieved by carefully selecting the building blocks and organic ligands containing appropriate functional groups through supramolecular interactions [1]. Such metal-organic coordination polymers have intriguing topological structures and potential applications in host–guest chemistry, electrical conductivity, catalysis, molecular magnets, nonlinear optics, gas storage, ion exchange, adsorption, phase separation, and antimicrobial activity [2, 3]. The ligand geometry and the coordination preference of the metal ions play important roles, as shown by silver coordination polymers [4, 5]. Silver(I) adopts linear, trigonal, and tetrahedral coordination environments and has high affinity to hard and soft donors. Organodiimines and heterocyclic aromatic compounds are good candidates for the construction of silver-organic coordination polymers because of their rich coordination modes [6, 7]. Hydrothermal reactions of silver salts and ligands gave rise to multidimensional topologies [8].

*Corresponding author. Email: safaaetaiw@hotmail.com

ISSN 0095-8972 print/ISSN 1029-0389 online
DOI: 10.1080/00958971003695529

This work constructs silver-containing supramolecular coordination polymers (SCPs) through the combination of supramolecular interactions. Two strategies can be applied for the construction of extended arrays of metal-containing molecules linked *via* supramolecular interactions, combining hydrogen bonds or other interactions with coordination chemistry, and with organometallic π-arene chemistry [7(i), 8(a)]. In this work, we focus on the former strategy by using benzoic acid derivatives and bipodal ligands with versatile coordination ability. The present synthetic approach utilizes the reaction of an Ag(I) and the bipodal ligands to form a 1-D linear chain, which then is extended to high-dimensional supramolecular networks *via* the coordination bonds or supramolecular interactions provided by benzoic acid derivatives.

2. Experimental

All chemicals and solvents were of analytical grade supplied by Aldrich or Merck and used as received. Microanalyses (C, H, N) were carried out with a Perkin-Elmer 2400 automatic elemental analyzer. The infrared (IR) spectra were recorded on a Perkin-Elmer 1430 Ratio Recording Infrared Spectrophotometer as KBr discs. The mass spectra were recorded on a GCMS-Finnigan SSQ 70000. The thermogravimetric analysis was carried out on a Shimadzu AT 50 thermal analyzer (under N_2). The electronic absorption spectra as solid matrices were measured on a Shimadzu (UV-3101PC) spectrometer and the fluorescence spectra as solid matrices were measured with a Perkin–Elmer (LS 50 B) spectrometer.

2.1. *Synthesis of {[Ag(4,4′-bpy) · H_2O](4-ab) · 2H_2O} (1)*

A solution of 25 mg (0.15 mmol) of $AgNO_3$ in 20 mL of H_2O was added dropwise, under gentle stirring, to 30 mg (0.18 mmol) of 4,4′-bipyridine (4,4′-bpy) and 20 mg (0.146 mmol) of 4-amino benzoic acid (4-aba) in 30 mL acetonitrile. This colorless solution was kept at room temperature; after 1 week, yellow prismatic crystals formed. After filtration, washing with water and overnight drying about 35 mg (54.6% referred to $AgNO_3$) of yellow crystals were obtained. Anal. Calcd (%) for **1** ($C_{17}H_{20}N_3O_5Ag$): C, 44.94; H, 4.40; N, 9.25.2. Found (%): C, 44.3; H, 4.2; N, 9.05.

2.2. *Synthesis of {[Ag(tbpe)]0.5(4-hb) · 3H_2O} (2)*

At room temperature, a solution of 42 mg (0.25 mmol) of $AgNO_3$ in 20 mL of H_2O was added dropwise with stirring to a solution containing 40 mg (0.21 mmol) of trans-1,2-bis(4-pyridyl)ethylene (tbpe) and 25 mg (0.25 mmol) of 4-hydroxy benzoic acid (4-hba) in 30 mL acetonitrile. A brown precipitate was formed and ammonia solution was added to dissolve this precipitate; after 1 week, brown prismatic crystals resulted. After filtration, subsequent washing with water and overnight drying about 55 mg (90% referred to $AgNO_3$) of brown crystals were obtained. Anal. Calcd (%) for **2** ($C_{31}H_{37}N_4O_9Ag_2$): C, 45.11; H, 4.48; N, 6.79. Found (%): C, 45.02; H, 4.3; N, 6.6.

2.3. *Synthesis of [$Ag_2(L)_2 \cdot (tph)$] (L = 4,4′-bpy, tbpe) (3,4) and {[$Ag_2(bpe)_2 \cdot (tph)$] · $2H_2O$} (5)*

An amount of 85 mg (0.5 mmol) of $AgNO_3$ in 20 mL of H_2O was added dropwise with stirring to a mixture of 66 mg (0.5 mmol) of terephthalate ions (tph) [0.5 mmol of terephthalic acid in 20 mL sodium hydroxide solution (1 mmol)] and 70 mg (0.42 mmol) of 4,4′-bpy, **3**, or 80 mg (0.43 mmol) of tbpe, **4** or 50 mg (0.27 mmol) of 1,2-bis(4-pyridyl)ethane (bpe), **5** in 20 mL hot acetonitrile. A brown precipitate was formed and ammonia solution was added to dissolve this precipitate. After 1 week, brown needle crystals of **3** or brown crystalline products of **4** and **5** were formed. Crystals **4** and **5** are not good enough for X-ray measurements. Attempts to obtain good quality crystals have not been successful to date. After filtration, subsequent washing with water and overnight drying about 80 mg (46% referred to $AgNO_3$) of brown crystals **3** or about 80 mg (45% referred to $AgNO_3$) of brown crystalline **4** or about 50 mg (26.7% referred to $AgNO_3$) of brown crystalline **5** were obtained. Anal. Calcd (%) for **3** ($C_{28}H_{20}N_4O_4Ag_2$): C, 48.58; H, 2.89; N, 8.09. Found (%): C, 48.3; H, 2.76; N, 7.91. Anal. Calcd (%) for **4** ($C_{32}H_{24}N_4O_4Ag_2$): C, 51.64; H, 3.21; N, 7.53. Found (%): C, 51.3; H, 3.1; N, 7.3. Anal. Calcd (%) for **5** ($C_{30}H_{32}N_4O_6Ag_2$): C, 45.94; H, 4.08; N, 7.14. Found (%): C, 46.12; H, 3.9; N, 8.1.

2.4. *Single crystal structure determination*

The structural measurements for **1**–**3** were performed on a Kappa CCD Enraf Nonius FR 90 four circle goniometer with graphite monochromated Mo-Kα radiation (λ Mo-Kα = 0.71073 Å) at 25 ± 2°C. All structures were resolved using direct methods and all of the non-hydrogen atoms were located from the initial solution or from subsequent electron density difference maps during the initial stages of the refinement. After locating all non-hydrogen atoms in each structure, the models were refined against F^2, first using isotropic and finally using anisotropic thermal displacement parameters. The positions of hydrogens were then calculated and refined isotropically, and the final cycle of refinements was performed. The crystallographic data for **1**–**3** are summarized in table 1. Selected bond distances and angles are given in tables 2–4.

3. Results and discussion

3.1. *Crystal structure of 1*

The asymmetric unit of **1** contains different molecules which consists of one silver, one 4,4′-bpy, one free 4-aminobenzoate (4-ab) and three waters (figure 1). The structure of **1** is slightly distorted linear $[Ag(4,4'\text{-bpy})]_n$ chains, 4-ab and water. Each Ag(I) is coordinated to two nitrogens from different, but crystallographically identical, 4,4′-bpy's in a slightly distorted linear fashion to form a chain of alternating Ag(I) and 4,4′-bpy (figure 2). Ag–N bond distance of 2.145 Å is typical Ag(I)–N_{py} coordination distance [9]. N30–Ag1–N5 bond angle of 173.11° is indicative of the presence of a distortion from linearity in **1**, which may be ascribed to a weak interaction between Ag(I) and an adjacent water, Ag–O31 = 2.703 Å. Thus, the coordination environment

Table 1. Crystallographic data and processing parameters for **1–3**.

	1	**2**	**3**
Empirical formula	$C_{17}H_{20}N_3O_5Ag$	$C_{31}H_{37}N_4O_9Ag_2$	$C_{28}H_{20}N_4O_4Ag_2$
Formula weight	453.87	824.6	691.612
Temperature (K)	298	298	298
Crystal system	Monoclinic	Orthorhombic	Monoclinic
Space group	$P2_1/m$	$F2dd$	$P2_1/c$
Unit cell dimensions (Å, °)			
a	8.2975(2)	10.3179(3)	14.6739(6)
b	17.5725(5)	17.9469(6)	7.1822(3)
c	9.9649(3)	34.194(2)	29.3464(3)
α	90.00	90.00	90.00
β	103.48(14)	90.00	102.435(3)
γ	90.00	90.00	90.00
Volume (Å^3), Z	1412.90(7), 4	6331.9(4), 18	3020.3(2), 4
Calculated density (g cm^{-3})	1.736	1.757	1.624
Absorption coefficient (Mo-Kα) (mm^{-1})	1.42	1.44	1.36
$F(000)$	772	3329	1456
$R_{(int)}$	0.023	0.022	0.039
Data/restraints/parameters	2309/0/196	1274/0/210	1991/0/128
Goodness-of-fit on F^2	4.662	3.052	10.427
Final R indices [$I > 3\sigma(I)$]	$R_1 = 0.088$, $wR_2 = 0.210$	$R_1 = 0.032$, $wR_2 = 0.063$	$R_1 = 0.161$, $wR_2 = 0.359$
R indices (all data)	$R_1 = 0.115$, $wR_2 = 0.213$	$R_1 = 0.058$, $wR_2 = 0.070$	$R_1 = 0.259$, $wR_2 = 0.370$

Table 2. Bond lengths (Å) and angles (°) of **1**.

Ag1–N5	2.157(6)	Ag1–C13	3.065(7)
Ag1–N30	2.151(6)	Ag1–Ag1^{xiii}	3.452(12)
Ag1–O31^{i}	2.703(5)		
Ag1–C13	3.070(6)		
Ag1–C19	3.032(6)	N5–Ag1–O31^{i}	91.43(2)
Ag1–C21	3.044(7)	N5–Ag1–N30	173.11(2)
Ag1–C25	3.071(5)	N30–Ag1–O31	91.97(2)
Ag1–O31^{i}	2.703(5)	Ag1–N30–C19	119.97(3)
C23–O28	1.262(12)	Ag1–N30–C13	122.56(3)
O8–C23	1.310(13)	Ag1–N5–C21	121.37(5)
O8–N29	2.981(3)	Ag1–N5–C25	122.93(5)
Hydrogen bonds			
O8–H14^{ii}	2.395(3)	O34–H22	2.968(3)
O8–H11	2.459(3)	O31–H21^{i}	2.559(3)
O8–H17	2.729(3)	O31–H19^{v}	2.541(3)
O8–H29B	2.040(3)	N29–H32B	2.216(3)
O28–H31A	2.773(3)	N5–H31B	2.580(6)
O28–H16	2.521(8)	Ag1–H31A^{i}	2.202(7)
O28–H31A	2.773(3)	Ag1–H31B^{i}	2.602(7)
O32–H29A	2.190(3)		

Symmetry codes: (i) $x-1$, $1/2-y$, $1/2+z$; (ii) $-1-x$, $1/2+y$, $3/2-z$; (v) $1/2+x$, $1/2-y$, $1/2-z$; (xiii) $1-x$, $-y$, $-1-z$.

around Ag(I) can also be described as slightly distorted T-shaped. The Ag–Ag and Ag–H bonding interactions as well as semi-coordinative interaction between Ag1 and oxygen of the water molecule from another chain (Ag1–Ag1 = 3.452 Å, Ag–H31B = 2.602 Å, and Ag1–O31 = 3.240 Å) cause pyramidization of the silver such

Table 3. Bond lengths (Å) and angles (°) of **2**.

Ag1–O3^{i}	2.785(13)	O3^{i}–Ag1–N5^{ii}	102.36(6)
Ag1–N5^{ii}	2.159(2)	O3^{i}–Ag1–N15	91.92(6)
Ag1–N15	2.144(2)	N5^{ii}–Ag1–N15	165.63(6)
Ag1–C16	3.064(3)	Ag1–N15–C25	121.34(6)
Ag1–C22^{ii}	3.058(2)	Ag1–N15–C16	121.20(6)
Ag1–C25	3.053(2)	Ag1–N5–C22	119.58(6)
O2–O3	2.664(2)	Ag1–N5–C24	122.68(6)
O2–C21^{iii}	1.296(3)		
O4–C6	1.256(2)		
Hydrogen bonds			
O4–H22	2.495(14)	O3–H25	2.556(15)
O4–H3A^{viii}	2.999(14)	O3–H22	3.028(15)
O4–H14^{iii}	2.557(14)	O3–H9A^{v}	2.941(13)
O4–H16^{viii}	2.875(15)	O3–H9B^{v}	2.505(14)
O18–H24	2.690(15)	O3–H2	2.162(13)
O18–H16	3.002(14)	O18–H9A	1.940
O9–H8	2.903(14)	O18–H9B	2.376
O9–H11	2.773(2)	O9–H14	2.967
O9–H14^{i}	2.967(2)	O4–H3B	1.935
O2–H17	2.577(11)	O18–H9A	1.940
O2–H13	2.441(15)	O3–H2	2.162
O2–H3B	2.903(14)	Ag1–H16	3.059(2)

Symmetry codes: (i) $x-1, 1/2-y, 1/2+z$; (ii) $-1-x, 1/2+y, 3/2-z$; (iii) $x-1/2, 1/2-y, 1/2-z$; (v) $1/2+x, 1/2-y, 1/2-z$; (viii) $1/2-x, y-1/2, 1/2+z$.

Table 4. Bond lengths (Å) and angles (°) of **3**.

Ag1–N11^{i}	2.166(10)	N11^{i}–Ag1–N36	178.5(4)
Ag1–N36	2.189(11)	N8–Ag2–N20	176.04(3)
Ag2–N8	2.139(9)	C43–N36–Ag1	120.07(3)
Ag2–N20	2.153(10)	C47–N36–Ag1	120.69(3)
C19–O27	1.280(6)	C23–N11–Ag1	118.05(3)
C19–O30	1.275(6)	C15–N11–Ag1	126.74(3)
C50–O5	1.331(6)	C38–N20–Ag2	119.76(3)
C50–O42	1.262(6)	C37–N20–Ag2	124.40(3)
		C4–N8–Ag2	125.00(3)
		C6–N8–Ag2	120.45(3)
Hydrogen bonds			
O5–H7	2.700	O27–H3	2.6843
O5–H17	2.639	O5–H14	2.598
O30–H4	2.680	O5–H10	2.931
O30–H15	2.669	O30–H22	2.749
O27–H38	2.935	O30–H14	2.2288
O27–H47	2.887		

Symmetry codes: (i) $x-1, 1/2-y, 1/2+z$.

that the angles of the trigonal planar geometry around silver deviate largely from 120° (table 2).

The structure of **1** consists of two chains arranged in ... ABAB ... fashion. Chain A is 1-D containing $[Ag(OH_2)\mu_2$-(4,4′-bpy)$]_n$ fragments. Chain B is constructed of uncoordinated 4-ab and two waters. The plane of chain B is out of the plane defined by

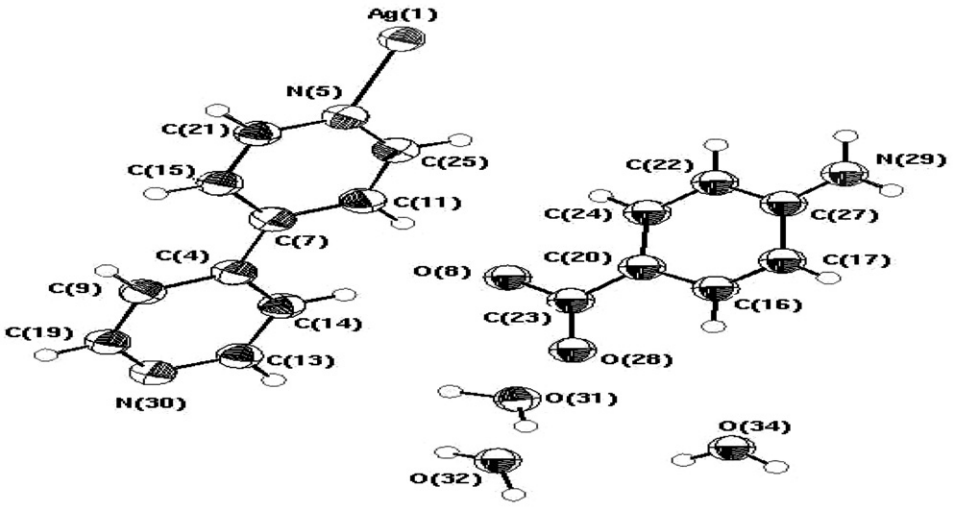

Figure 1. ORTEP plot showing the asymmetric unit of **1** with atom labeling scheme.

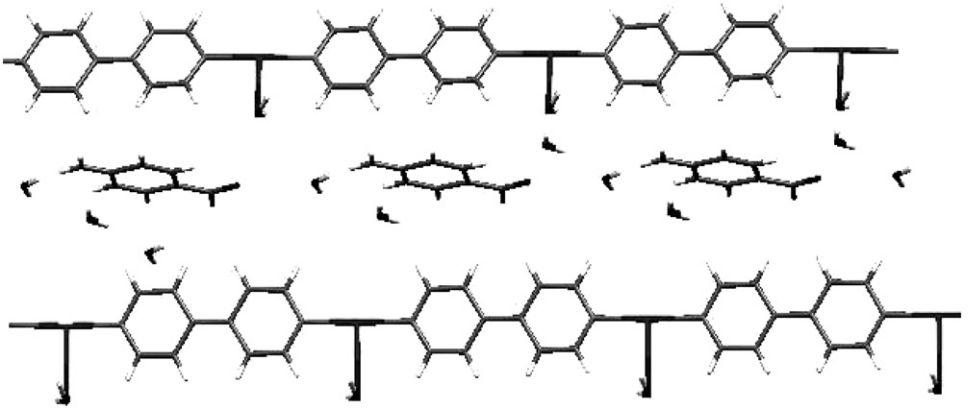

Figure 2. A view of the expanded structure of **1** along the *a*-axis.

the 1-D chain A by an angle equal to 78.35°. Two 1-D chains A are linked to each other by π–π interactions, 3.714 Å, and hydrogen bonding forming a parallel pair. Each two parallel [Ag(OH_2)μ_2(4,4′-bpy)] chains are stacked by face-to-face π–π interactions of the pyridyl rings of 4,4′-bpy and by hydrogen bonds between the coordinated water and 4,4′-bpy, N5-H31B = 2.58 Å, O31–H25 = 3.40 Å, developing a 2-D layer. This layer is further stabilized by argentophilic interaction at 3.452 Å. The pyridine rings of 4,4′-bpy are not coplanar as one ring is tilted out of the plane defined by the other one by an angle of 5.98°.

Two B chains are linked by hydrogen bonds between water and 4-ab forming a 2-D layer (table 2). There are also short contacts between oxygen of carboxylate and oxygen of free water, O28–O32 = 3.008 Å.

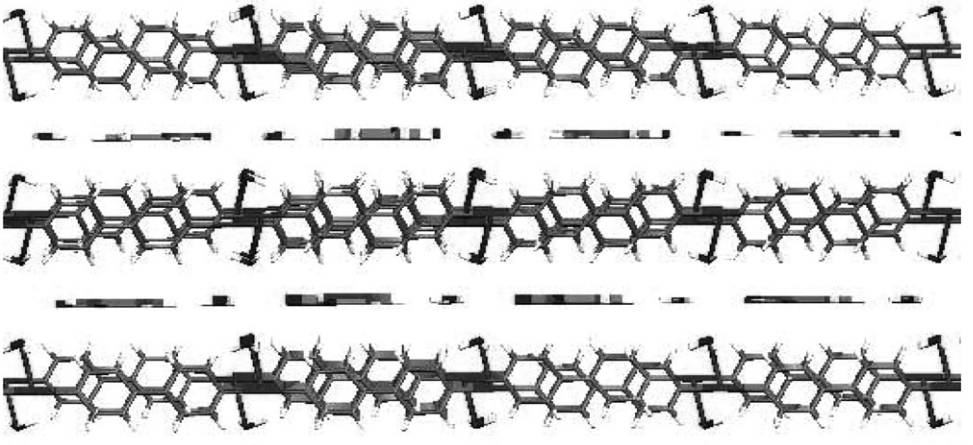

Figure 3. Visualization of the 3-D network showing channels in **1** along the *a*-axis.

The structure of **1** is packed as a 3-D open framework creating channels, where the cationic layers of chain A accommodate the anionic layer B (figure 3). In this case, chains A and B are linked by hydrogen bonding. These hydrogen bonds are formed between oxygens of free 4-ab and hydrogens of 4,4′-bpy (O8–H14 = 2.394 Å, O8–H11 = 2.459 Å), and also between oxygens and nitrogens of another free 4-ab and hydrogens of coordinated water and the hydrogens of 4,4′-bpy (O28–H31 = 2.773 Å), table 2. Furthermore, there is a strong hydrogen bond between hydrogens of coordinated water in $[Ag(OH_2)\mu_2(4,4'\text{-bpy})]_\infty$ and nitrogens of 4,4′-bpy in another chain (N5–H31B = 2.580 Å). Thus, water plays an essential role in connecting the layers as they thread along the sides of the layers developing a 3-D network.

3.2. *Crystal structure of 2*

The asymmetric unit of **2** consists of one silver, one tbpe, half of 4-hydroxybenzoate (4-hb) and three free waters (figure 4). The silver is distorted linear, coordinated to two nitrogens of two tbpe, N5–Ag1–N15 = 165.66°, forming the main building block of **2**. The deviation from linearity is caused by the close contact between Ag1 and oxygen of free water, Ag1–O3 = 2.786 Å, and hydrogen bonds between oxygen of the free water and hydrogen of tbpe, O3–H25 = 2.556 Å and O3–H22 = 3.028 Å, as well as Ag–H interaction, Ag1–H3A = 1.899 Å. The silver is strongly bonded to nitrogens of two tbpe; Ag1–N15 and Ag1–N5 bond lengths are 2.144 and 2.159 Å, respectively, table 3, typical for Ag–N coordination [9].

The main building blocks $[Ag\mu_2(tbpe)]_nH_2O$ form 1-D chains, which are arranged in two different planes with one chain out of the plane defined by the other chain by an angle of 36.57°.

The analysis of **2** reveals attractive interactions between adjacent $[Ag\mu_2(tbpe)]_nH_2O$ chains are hydrogen bonds, 2.556–3.002 Å, Ag...tbpe contacts, 3.387 Å, and π–π interactions between ethylene groups of tbpe ligands and pyridine rings of

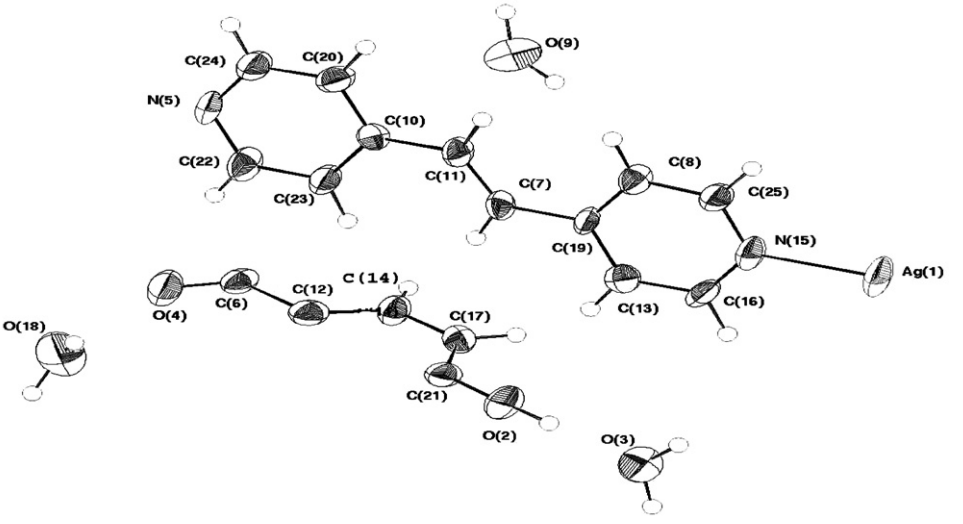

Figure 4. ORTEP plot showing an asymmetric unit of **2** with atom labeling scheme.

another tbpe, 3.441–3.753 Å. There are no π–π interactions between pyridine rings of tbpe as the closed separation distance between adjacent rings is 5.053 Å. Furthermore, there are no argentophilic interactions as the closest Ag···Ag separation is 5.209 Å. The Ag–π and π–π interactions further extend the $[Ag\mu_2(tbpe)]_nH_2O$ chains into a 2-D layer. The layers also involve the contacts between silvers and oxygens of water and the hydrogen bonds between these water molecules and hydrogens of tpbe (table 3).

The network of **2** consists of $[Ag\mu_2(tbpe)]_nH_2O$ in chains and the free chain of 4-hb with two waters. This free chain is out of the plane defined by the 1-D chain $[Ag\mu_2(tbpe)]_nH_2O$ by 85.37°. The chain constructed by free 4-hb and uncoordinated water is formed *via* hydrogen bonds between hydrogen of hydroxyl of 4-hb and oxygen of the carboxylate of another 4-hb and between 4-hb and uncoordinated water (table 3).

The $[Ag(tbpe)]_nH_2O$ chains interact with another chain of free 4-hb and water by hydrogen bonding, generating a 3-D SPC with open framework having extended channels. The channels accommodate layers of 4-hb and water (figure 5). Strong intermolecular hydrogen bonds exist between carboxylate and hydroxyl of free 4-hb and hydrogen of tbpe (O4–H22 = 2.495 Å, O2–H13 = 2.441 Å), and also between oxygen of water and hydrogen of tbpe (table 3). Water plays an essential role in connecting the layers as they thread along the sides of the layers, creating a 3-D network.

3.3. *Crystal structure of 3*

The asymmetric unit of **3** contains two crystallographically different silvers, two 4,4′-bpy molecules and one free tph (figure 6). The two silvers have slightly distorted linear geometry, with each silver coordinated to two nitrogens of two different 4,4′-bpy, N8–Ag2–N20 = 176.1° and N11–Ag1–N36 = 178.5°. The silvers are strongly bonded to nitrogen with Ag2–N stronger than Ag1–N.

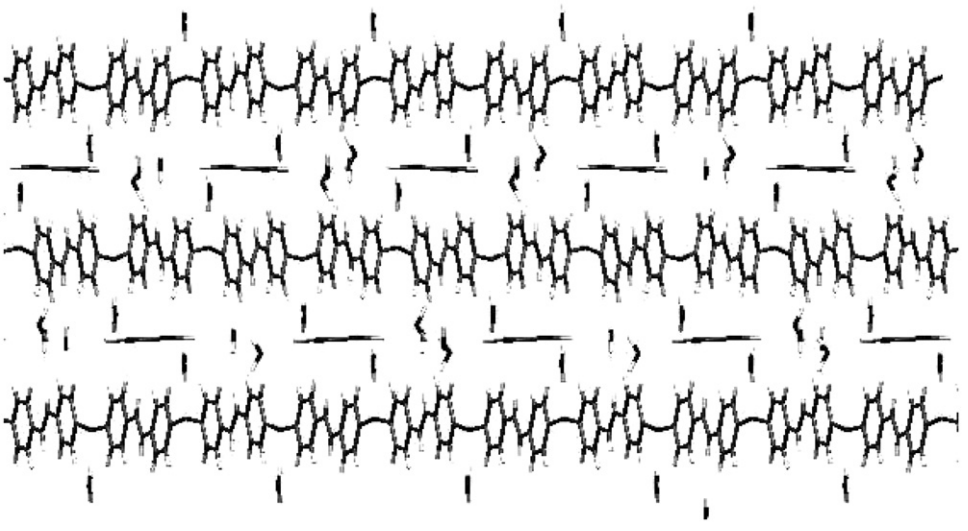

Figure 5. 3-D network showing channels in **2** along the *b*-axis.

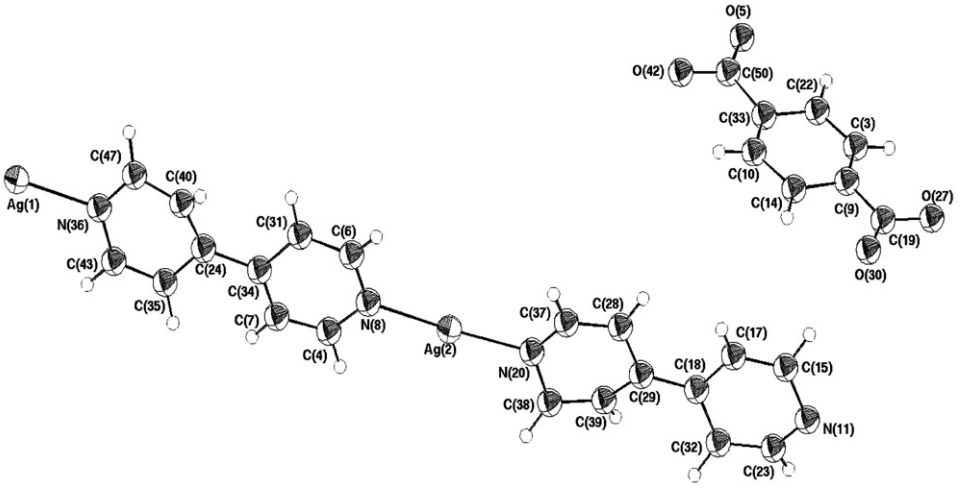

Figure 6. ORTEP plot showing an asymmetric unit of **3** with atom labeling scheme.

The structure of **3** consists of two chains arranged in . . . ABAB . . . fashion. Chain A, contains $[Ag(4,4'\text{-bipy})]_n$, while chain B contains uncoordinated tph ions. Chain B is perpendicular to the 1-D chain of $[Ag(4,4'\text{-bipy})]_n$ with an angle of 89.6°.

Each pair of $[Ag\mu_2(4,4'\text{-bipy})]_n$ chains is significantly shifted with respect to the other, forming interwoven infinite $[Ag\mu_2(4,4'\text{-bipy})]_n$ chains. The analysis of **3** reveals the attractive interaction between the adjacent $[Ag(4,4'\text{-bipy})]_n$ chains by $Ag\cdots\pi$ contacts between Ag and pyridine, 3.508 Å; π–π stacking between interwoven adjacent pyridine rings, C32–C15 = 3.48 Å and C17–C23 = 3.464 Å. There are no argentophilic

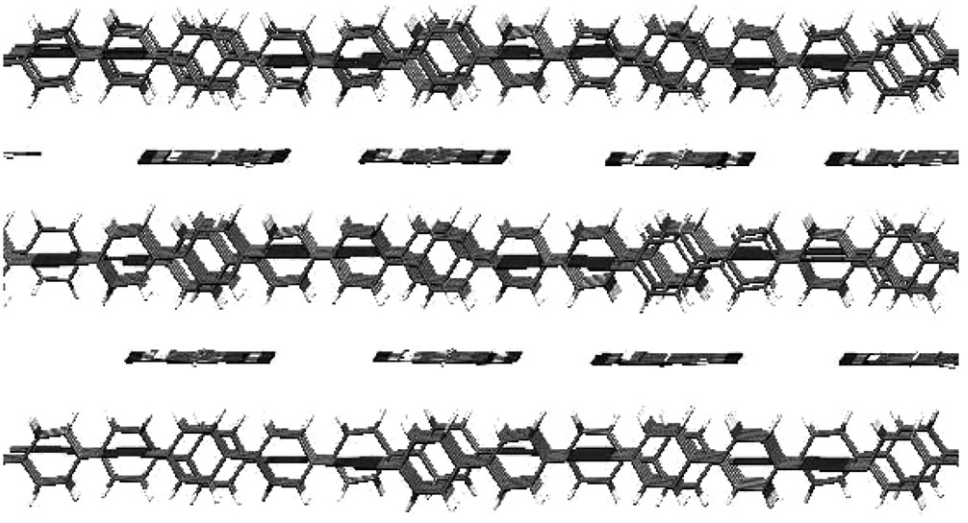

Figure 7. Interwoven 3-D network showing channels in **3** along the *b*-axis.

interactions as the closest Ag–Ag separation is 4.946 Å. The Ag–π and π–π interactions further extend the $[Ag(4,4'\text{-bipy})]_n$ chains into a 2-D layer.

Chain B of uncoordinated tph is constructed *via* hydrogen bonds between the oxygen of carboxylate of tph and hydrogens of another tph, O30–H22 = 2.749 Å, O5–H14 = 2.598 Å and O5–H10 = 2.931 Å (table 4).

A and B are further linked by hydrogen bonds generating a 3-D network structure. Hydrogen bonds are formed between the oxygens of tph and hydrogens of 4,4′-bpy (table 4). Thus, tph are linkers of adjacent $[Ag\mu_2(4,4'\text{-bipy})]_n$ layers and consolidate the structural framework.

The extended structure of **3** is interwoven forming 3-D network *via* hydrogen bonding, metal–π and $\pi\cdots\pi$ interactions (figure 7). The packing of **3** creates channels with the Ag···Ag separation distance between the adjacent layers equal to 8.762 Å. These channels accommodate chain B of free tph ions (figure 7).

3.4. *Infrared spectra of 1–5*

The IR spectra of **1** and **2** display a strong broad band at 3420 and 3395 cm^{-1}, respectively, corresponding to stretching of water combined with stretching vibrations of amino and hydroxy groups. This band shifts to lower wave numbers than the free ligands, suggesting the formation of strong hydrogen bonds. Bands at 2429, 1867 cm^{-1} and 2361, 1849 cm^{-1} in **1** and **2**, respectively, are assigned to strong hydrogen bonding of the type (N···H–O) of free benzoic acid derivatives and bipodal ligands. The characteristic bands of the carboxylate groups appear at 1535, 1378 cm^{-1} and at 1595, 1378 cm^{-1} for **1** and **2**, respectively, suggesting the involvement of the carboxylate group in strong intermolecular hydrogen bonds. The bipodal ligands (Supplementary material) show shifts to lower wave numbers than the free ligands due to the

coordination to silver and due to the formation of hydrogen bonds between the oxygen of 4-ab and 4-hb with the water and hydrogen of the bipodal ligands.

The IR spectra of **3**–**5** show bands characteristic of tph and the bipodal ligands, 4,4′-bpy, tbpe and bpe (Supplementary material). These bands shift to lower wave numbers than those of the free ligands due to the formation of hydrogen bonds.

3.5. *Thermogravimetric analyzes*

The thermal decomposition thermograms of **1**–**5** show broad similarity, but are not identical; first dehydration occurs followed by the loss of free benzoic acid derivatives and finally the decomposition of the organic bidentate ligand. After complete thermolysis, the calculated and observed percentages of the residues are coincident with metallic silver.

The thermogram of **1** exhibits two steps in the temperature range 90–150°C and 150–170°C corresponding to the release of two free waters and one coordinated water, respectively; the three waters in **2** are released in one step at 90–150°C. As network structures of **1**–**5** lose solvent, they lose uncoordinated 4-ab, 4-hb and tph, *via* breaking the hydrogen bonds up to 170°C reflecting the strong hydrogen bonding and supramolecular forces constructing the network structures of **1**–**5**.

3.6. *Mass spectra of 4 and 5*

The constitutions of **4** and **5** are established by mass spectrometry (Supplementary material). The mass spectra exhibit peaks at m/z 740 and m/z 827 corresponding to the molecular weights of **4** and **5**, further support of the structure suggested by elemental analyzes. Fragmentation of bpe is illustrated in "Supplementary material". The interpretations of the mass spectra are listed in "Supplementary material". Thus, mass spectra of **4** and **5** confirm the presence of the bipodal ligands (tbpe, bpe) and tph fragments and the molecular formula. Also, they support the polymeric nature of (Ag-L) building blocks.

3.7. *Electronic absorption and emission spectra of 1–5*

The electronic absorption spectra of **1**–**5** from 225 to 450 nm depend on the organic ligand (Supplementary material). The spectrum of **1** resembles that of **3** as both contain 4,4′-bpy. Bands at 236 and 260 nm in **1** and at 232 and 257 nm in **3** are due to $^1L_a \leftarrow {}^1A$ and $^1L_b \leftarrow {}^1A$ transitions, which are bathochromicly shifted from those in benzene. Bands at 280 nm in **1** and 275 nm in **3** are due to $^1L_b \leftarrow {}^1A$ transitions in 4-ab and tph, respectively. The bathochromic shift is due to the interaction resonance of the para-disubstituents of benzene. Bands at 325 nm in **3** and 326–365 nm in **1** correspond to the intermolecular charge transfer within tph and 4-ab, respectively. The spectrum of **3** does not show any bands due to n–π^* transitions, due to the strong hydrogen bonding of carboxylates; however, the spectrum of **1** shows n–π^* at 410 nm. The spectra of **2**, **4,** and **5** display, in addition to the ^1L_a (223–230 nm) and ^1L_b (255 and 285 nm) bands, a band at 305 nm in **2**, 315 nm in **4** and 312 in **5** corresponding to $^1B \leftarrow {}^1A$ which resembles that of stilbene. The spectra of **2**, **4** and **5** display additional

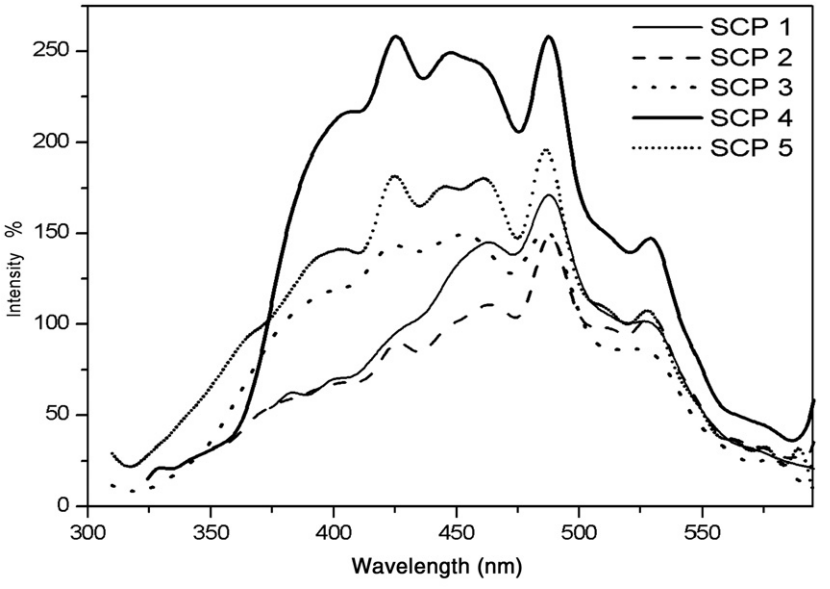

Figure 8. Solid-state emission spectra of **1**–**5** upon excitation at 300 nm.

bands at 340–325 nm due to intermolecular charge transfer within the organic ligand. The absence of bands due to n–π^* is due to the strong hydrogen bonding.

The emission spectra of **1**–**5** resemble those of the bipodal ligands exhibiting vibrational bands around 420, 450, 480, and 530 nm (figure 8). The higher energy bands correspond to the lowest (π–π^*) and close lying n–π^* states; long wavelength bands are due to metal-to-ligand charge-transfer (MLCT) or metal-centered transitions of the type $4d^{10} \rightarrow 4d^9\ 5s^1$ and $4d^{10} \rightarrow 4d^9\ 5p^1$ on silver(I).

4. Conclusion

Self-assembly of silver(I) ions with bipodal ligand (4,4′-bpy, tbpe or bpe) in the presence of organic ligand (4-aba, 4-hba or tph) as structure directing agents afford five 3-D SPCs. The mass spectra of **4** and **5** indicated polymers. The bipodal ligand is coordinated to silver forming 2-D cationic layers (A), while the organic and the solvent molecules thread between these layers forming 2-D anionic layers (B) *via* hydrogen bonds and π–π stacking interactions. Hydrogen bonds and π–π stacking between these layers form 3-D networks. Organic ligands containing nitrogen and carboxylate are preferred building blocks for preparing 3-D SCPs *via* hydrogen bonding. This is supported by the formation of 2-D network containing 1-D channels of $[Ag_2(bpdc)]_n$ ($H_2bpdc = 2,2'$-bipyridyl-3,3′-dicarboxylic acid) [10] and the 2-D network containing Ag-bte tubular structures (bte = 1,2-bis(1,2,3-triazole-1-yl)ethane [11]. Coordination compounds **1**–**5** are formed at room temperature compared with the 2-D and 3-D silver-organic coordination polymers $[Ag(NH_2\text{-}Bpt)\cdot NO_3]_n$ [12] and $[Ag(L^1)\cdot(m\text{-}Hbdc)]$, $\{Ag(L^1)_2\cdot(p\text{-}bdc)]\cdot 8H_2O\}$, $\{[Ag(Hbtc)(L^1)][Ag(L^1)]\cdot 2H_2O\}$

and $\{[Ag_2(L^2)_2](OH\text{-}bdc)_2 \cdot 4H_2O\}$ [13] under hydrothermal conditions. At room temperature, **1**–**5** display strong photoluminescence.

Supplementary material

CCDC nos 723257–723259 contain the supplementary crystallographic data for **1**–**3**. These data can be obtained free of charge *via* http://www.ccdc.cam.ac.uk/conts/retrieving.html, or from the Cambridge Crystallographic Data Centre, 12 Union Road, Cambridge CB2 1EZ, UK; Fax: +44-1223-336033 or Email: deposit@ccdc.cam.ac.uk.

References

[1] (a) C.M.R. Juan, B. Lee. *Coord. Chem. Rev.*, **183**, 43 (1999); (b) M.-C. Tse, K.-K. Cheung, M.C.-W. Chan, C.-M. Che. *Chem. Commun.*, 3245 (1998); (c) M. Tadokoro, K. Isobe, H. Uekusa, Y. Ohashi, J. Toyoda, K. Tashiro, K. Nakasujhi. *Angew. Chem. Int. Ed.*, **38**, 95 (1999); (d) Y.-L. Wang, Q.-Y. Liu, L. Xu. *CrystEngComm.*, **10**, 1667 (2008); (e) Q.-Y. Liu, L. Xu. *Eur. J. Inorg. Chem.*, 3458 (2005); (f) Q.-Y. Liu, D.-Q. Yuan, L. Xu. *Cryst. Growth Des.*, **7**, 1832 (2007); (g) H. Wu, X.-W. Dong, H.-Y. Liu, J.-F. Ma, S.-L. Li, J. Yang, Y.-Y. Liu, Z.-M. Su. *Dalton Trans.*, 5331 (2008); (h) P.-Y. Cheng, C.-Y. Chen, H.M. Lee. *Inorg. Chim. Acta*, **362**, 1840 (2009); (i) T.S. Lobana, R. Sharma, R.J. Butcher. *Polyhedron*, **28**, 1103 (2009); (j) S.E.H. Etaiw, D.M. Abd El-Aziz, M.S. Ibrahim, A.S. Badr El-din. *Polyhedron*, **28**, 1001 (2009).

[2] (a) C. Janiak. *Dalton Trans.*, 2781 (2003); (b) C.-D. Wu, W.-B. Lin. *Angew. Chem. Int. Ed.*, **44**, 1958 (2005); (c) G.V. Oshovsky, D.N. Reinhoudt, W. Verboom. *Angew. Chem. Int. Ed.*, **46**, 2366 (2007); (d) O.M. Yaghi, M. O'Keeffe, N.W. Ockwig, H.K. Chae, M. Eddaoudi, J. Kim. *Nature*, **423**, 705 (2003); (e) R. Custelcean, B.A. Moyer. *Eur. J. Inorg. Chem.*, 1321 (2007); (f) L. Pan, D.H. Olson, L.R. Ciemnolonski, R. Heddy, J. Li. *Angew. Chem. Int. Ed.*, **45**, 616 (2006); (g) S.-L. Zheng, X.-M. Chen. *Aust. J. Chem.*, **57**, 703 (2004); (h) U. Mueller, M. Schubert, F. Teich, H. Puetter, K. Schierle-Arndt, J. Pastré. *J. Mater. Chem.*, **16**, 626 (2006); (i) D. Maspoch, D. Ruiz-Molina, J. Veciana. *Chem. Soc. Rev.*, **36**, 770 (2007); (j) D. Maspoch, D. Ruiz-Molina, J. Veciana. *J. Mater. Chem.*, **14**, 2713 (2004); (k) S.R. Batten, K.S. Murray. *Coord. Chem. Rev.*, **246**, 103 (2003); (l) G. Férey. *Chem. Soc. Rev.*, **37**, 191 (2008); (m) S. Bureekaew, S. Shimomura, S. Kitagawa. *Sci. Technol. Adv. Mat.*, **9**, art. no. 014108 (2008).

[3] (a) O.R. Evans, W. Lin. *Acc. Chem. Res.*, **35**, 511 (2002); (b) S. Kitagawa, R. Kitaura, S. Noro. *Angew. Chem. Int. Ed.*, **43**, 2334 (2004); (c) S.L. James. *Chem. Soc. Rev.*, **32**, 276 (2003); (d) Q.R. Fang, G.S. Zhu, Z. Jin, M. Xue, X. Wei, D.J. Wang, S.L. Qiu. *Angew. Chem. Int. Ed.*, **45**, 6126 (2006); (e) W.G. Wang, A.J. Zhou, W.X. Zhang, M.L. Tong, X.M. Chen, M. Nakano, C.C. Beedle, D.N. Hendrickson. *J. Am. Chem. Soc.*, **129**, 1014 (2007); (f) M.A.M. Abu-Youssef, V. Langer, Lars Öhrström. *Dalton Trans.*, 2542 (2006); (g) R.-Q. Zou, H. Sakurai, Q. Xu. *Angew. Chem. Int. Ed.*, **45**, 2542 (2006); (h) L. Yi, B. Ding, B. Zhao, P. Cheng, D.Z. Liao, S.P. Yan, Z.H. Jiang. *Inorg. Chem.*, **43**, 33 (2004); (i) J.M. Zheng, S.R. Batten, M. Du. *Inorg. Chem.*, **44**, 3371 (2005); (j) P.V. Bernhardt, F. Bozoglián, B.P. Macpherson, M. Martínez. *Coord. Chem. Rev.*, **249**, 1902 (2005).

[4] (a) D. Sun, R. Cao, W. Bi, J. Weng, M. Hong, Y. Liang. *Inorg. Chim. Acta*, **357**, 991 (2004); (b) S.L. Zheng, M.L. Tong, X.L. Yu, X.M. Chen. *J. Chem. Soc., Dalton Trans.*, 586 (2001); (c) D. Sun, R. Cao, W. Bi, X. Li, Y. Wang, M. Hong. *Eur. J. Inorg. Chem.*, 2144 (2004); (d) F.-T. Xie, H.-Y. Bie, L.-M. Duan, G.-H. Li, X. Zhang, J.-Q. Xu. *J. Solid State Chem.*, **178**, 2858 (2005).

[5] (a) W. Su, M. Hong, J. Weng, R. Cao, S. Lu. *Angew. Chem. Int. Ed.*, **39**, 2911 (2000); (b) P. Vaqueiro, A.M. Chippindale, A.R. Cowley, A.V. Powell. *Inorg. Chem.*, **42**, 7846 (2003); (c) A.P. Côté, G.K.H. Shimizu. *Inorg. Chem.*, **43**, 6663 (2004); (d) Q.M. Wang, T.C.W. Mak. *Inorg. Chem.*, **42**, 1637 (2003); (e) S.L. Zheng, M.L. Tong, R.W. Fu, X.M. Chen, S.W. Ng. *Inorg. Chem.*, **40**, 3562 (2001); (f) S.L. Zheng, M.L. Tong, X.M. Chen, S.W. Ng. *J. Chem. Soc., Dalton Trans.*, 360 (2002).

[6] (a) M.L. Tong, X.M. Chen, B.H. Ye. *Inorg. Chem.*, **37**, 5278 (1998); (b) K. Singh, J.R. Long, P. Stavropoulos. *J. Am. Chem. Soc.*, **119**, 2942 (1997); (c) M.E. Chapman, P. Ayyappan, B.M. Foxman, G.T. Yee, W. Lin. *Cryst. Growth Des.*, **1**, 159 (2001); (d) M.L. Tong, L.J. Li, K. Mochizuki, H.C. Chang, X.M. Chen, Y. Li, S. Kitagawa. *Chem. Commun.*, 428 (2003); (e) A.D. Burrows, M.F. Mahon, M.T. Palmer. *J. Chem. Soc., Dalton Trans.*, 1941 (1998); (f) T. Dorn, K.M. Fromm, C. Janiak. *Aust. J. Chem.*, **59**, 22 (2006); (g) O.-S. Jung, Y.I. Kim, Y.-A. Lee, S.W. Kang, S.N. Choi. *Cryst. Growth Des.*, **4**, 23 (2004).

[7] (a) C.Y. Chen, J.Y. Zeng, H.M. Lee. *Inorg. Chim. Acta*, **360**, 21 (2007); (b) R.S. Rarig Jr, J. Zubieta. *Inorg. Chim. Acta*, **319**, 235 (2001); (c) S. Qin, S. Lu, Y. Ke, J. Li, X. Wu, W. Du. *Solid State Sci.*, **6**, 753 (2004); (d) J.C. Mareque Rivas, L. Brammer. *Coord. Chem. Rev.*, **183**, 43 (1999); (e) M.-C. Tse, K.-K. Cheung, M.C.W. Chan, C.-M. Che. *Chem. Commun.*, 3245 (1998); (f) M. Tadokoro, K. Isobe, H. Uekusa, Y. Ohashi, J. Toyoda, K. Ashiro, K. Nakasujhi. *Angew. Chem. Int. Ed.*, **38**, 95 (1999); (g) M. Du, C.-P. Li, X.-J. Zhao. *Cryst. Growth Des.*, **6**, 335 (2006); (h) L. Carlucci, G. Ciani, D.M. Proserpio, S. Rizzato. *CrystEngComm.*, **22**, 121 (2002); (i) F.-F. Li, J.-F. Ma, S.-Y. Song, J. Yang. *Cryst. Growth Des.*, **6**, 209 (2006).

[8] (a) D. Sun, R. Cao, Y. Sun, W. Bi, X. Li, Y. Wang, Q. Shi, X. Li. *Inorg. Chem.*, **42**, 7512 (2003); (b) C.-J. Wang, Y.-Y. Wang, H. Wang, G.-P. Yang, G.-L. Wen, M. Zhang, Q.-Z. Shi. *Inorg. Chem. Commun.*, **11**, 843 (2008); (c) Y.-B. Dong, G.-X. Jin, M.D. Smith, R.-Q. Huang, B. Tang, H.-C. Zur-Loye. *Inorg. Chem.*, **41**, 4909 (2002); (d) L.S. Sowa, T. Konaka, H. Suenaga, Y. Maekawa, M. Mizutani, T. Ning, G.L. Munakata. *Inorg. Chem.*, **44**, 1031 (2005); (e) S. Zhang, Z. Wang, H. Zhang, Y. Cao, Y. Sun, Y. Chen, C. Huang, X. Yu. *Inorg. Chim. Acta*, **360**, 2704 (2007); (f) F.-F. Li, J.-F. Ma, S.-Y. Song, J. Yang, Y.-Y. Liu, Z.-M. Su. *Inorg. Chem.*, **44**, 9374 (2005).

[9] (a) R. Wang, M. Hong, J. Luo, F. Jiang, L. Han, Z. Lin, R. Cao. *Inorg. Chim. Acta*, **357**, 103 (2004); (b) A.N. Khlobystov, A.J. Blake, N.R. Champness, D.A. Lemenovskii, A.G. Majouga, N.V. Zyk, M. Schröder. *Coord. Chem. Rev.*, **222**, 155 (2001); (c) M. Munakata, L.P. Wu, T. Kuroda-Sowa. *Adv. Inorg. Chem.*, **46**, 173 (1999); (d) C. Janiak. *J. Chem. Soc., Dalton Trans.*, 3885 (2000).

[10] X.-L. Chen, Y.-J. Yao, H.-M. Hu, S.-H. Chen, F. Fu. *J. Coord. Chem.*, **62**, 2147 (2009).

[11] B. Ding, E.-C. Yang, X.-J. Zhao, X.G. Wang. *J. Coord. Chem.*, **62**, 287 (2009).

[12] Q.-G. Zhai, J.-P. Niu, M.-C. Hu, Y. Wang, W.-J. Ji, S.-N. Li, Y.-C. Jiang. *J. Coord. Chem.*, **62**, 2927 (2009).

[13] Y.-Y. Liu, J.-C. Ma, L.-P. Zhang, J.-F. Ma. *J. Coord. Chem.*, **61**, 3583 (2008).